Journal of Young Pharmacists, 2023; 15(4):659-670.
https://www.jyoungpharm.org

Original Article

Bioactive Compounds from *Momordica charantia*, *Nigella sativa*, and *Anethum graveolens* against Metabolic Syndrome: Untangling the Complex Relationship

Rajashekar S. Chavan, Nayeem A. Khatib*, Vishal S. Patil

Department of Pharmacology, KLE College of Pharmacy, Belagavi, KLE Academy of Higher Education and Research, Nehru Nagar, Belagavi, Karnataka, INDIA.

ABSTRACT

Background: *Momordica charantia* (MC), *Nigella sativa* (NS), and *Anethum graveolens* (AG) are widely utilized vegetables and as an herbal medicines, despite widespread use, there is no evidence of molecular mechanisms of compound-protein-pathway interaction for the treatment of metabolic syndrome (MetS). **Materials and Methods:** Reported phytochemicals were collated from the botanical databases and SwissTargetPrediction was utilized to predict likely protein targets. Both the STRING and KEGG databases were used to infer the protein target pathway analysis. Cytoscape v3.6.1 was employed to build the compound-protein-pathway network. AutoDock vina executed through POAP pipeline was employed for therapeutic target and compounds docking study. Molecular dynamics was performed by GROMACS. **Results:** 34, 19, 34 phytocompounds from three plants MC, NS, and AG were predicted to target 30, 30, 28 protein targets and these targets modulated 20, 18, 22 molecular pathways respectively involved in metabolic syndrome. Neuroactive ligand-receptor interaction, Calcium, cGMP-PKG, cAMP, AMPK, PI3K-Akt, PPAR, Metabolic signaling pathways, etc were modulated by compounds. PPARG was hub gene within the network. Nigellidine from NS, Nigellimine-N-Oxide from NS, Cryptoxanthin from MC scored lowest BE with PPARG (-7.5kcal/mol), FABP1 (-8.8kcal/mol), and HMGCR (-7.1kcal/mol) protein targets respectively. MD simulation for 100ns revealed stable interactions of phytocompounds comparable to standard molecules. **Conclusion:** The current study identified multi-compounds containing enhanced fraction of MC, NS, and AG could be the effective therapy regimen for diabetes, obesity, and MetS.

Keywords: *Anethum graveolens*, Metabolic syndrome, *Momordica charantia*, Molecular dynamcis, Network Pharmacology, *Nigella sativa*.

Correspondence:
Dr. Nayeem A. Khatib
Head of Department of Pharmacology, KLE College of Pharmacy, Belagavi, KLE Academy of Higher Education and Research, Nehru Nagar, Belagavi 590010, INDIA.
Email: khatibnayeem@hotmail.com

Received: 13-07-2023;
Revised: 13-08-2023;
Accepted: 26-08-2023.

INTRODUCTION

Metabolic Syndrome (MetS) is characterized by a cluster of risk factors for cardiovascular disease, high blood pressure, obesity, and Type 2 Diabetes Mellitus (T2DM): dyslipidemia, Insulin Resistance (IR), Hypertension (HTN), and abdominal fat because of both genetic and acquired factors.[1,2] The rate of obesity increase is much faster than the discovery of effective treatments for obesity and metabolic illnesses.[3] Obesity and T2DM often go along over time. Stats show Obesity affects 60–90% of T2DM patients.[4,5] Currently, the major portion of prescriptions for the pharmacotherapy of obesity and T2DM includes PPAR-γ agonists, statins, insulin sensitizers, etc. are utilized for the management of T2DM, obesity, and MetS.[6] Anti-diabetic thiazolidinediones primarily act on the PPAR-γ resulting in transcription of genes involved in glucose elimination and they lower plasma glucose, triglycerides, and free fatty acids.[7] However, these agents cause "ketoacidosis, pancreatitis, genital mycosis, neuropathy risk, nausea, and vomiting" and these compounds have multiple limitations since they target a particular protein molecule that may influence other proteins.[8] Hyperglycemia symptoms may vary with diabetes duration, although metabolic alterations might affect them.[9] Hence, the WHO recommends testing novel T2DM hypoglycemic and anti-obese medications from herbs, and previous experimental and computational studies have identified lead hit compounds as anti-diabetic drugs from herbs.

Multiple bioactives in plant extracts work via the "multi compound-multi protein-multi pathway".[10] Newer drug development methods utilize an *in silico* methodologies[11] to predict the probable intermolecular interaction of compounds with protein targets and whether the compounds will bind to the respective binding site of the target and produce its best fit.[11,12] In

DOI: 10.5530/jyp.2023.15.91

the present study, we collected bioactives from three important medicinal plants and well-known vegetables, viz., *Momordica charantia* (MC), *Nigella sativa* (NS), and *Anethum graveolens* (AG), from herb databases and literature and processed them for *in silico* target identification by SwissTargetPrediction; gene set pathway enrichment and network analysis by STRING and KEGG databases; followed by molecular docking and dynamic studies to infer the compounds-proteins intermolecular interaction and their stability, respectively. Interestingly, the study identified major phytocompounds from these three plants to modulate therapeutic targets viz., PPARG-γ, FABP1, and HMGCR and also to regulate molecular pathways viz., Neuroactive ligand-receptor interaction, Calcium, cGMP-PKG, cAMP, AMPK, PI3K-Akt, PPAR, Metabolic signaling pathways involved in T2DM, obesity, and MetS-associated hypertension, and cardiovascular disease.

MATERIALS AND METHODS

Collection and target identification of bioactives form MC, NS, and AG

The reported bioactives from MC, NS, and AG were collected from the phytochemical databases such as phytochemical interaction DB, Dr. Dukes DB, IMPPAT,[13] and published original articles. Each compound's canonical SMILES were queried into the SwissTargetPredcition[14] server to retrieve the probable protein targets.

Gene set pathway and network analysis

The Search Tool for the Retrieval of Interacting Genes/Proteins v11.0 (STRING;[15] https://string-db.org) and its annotated tool KEGG[16] pathway database (https://www.genome.jp/kegg/pathway.html) have been employed to find bioactives influencing enriched DM, obesity, and MetS molecular pathways. Cytoscape v3.6.1 was utilized to create the compound-protein-pathway network.[17] The edge count metric and degree-sorted circular layout were implemented to detect highly modulated targets and pathways within the network.

Molecular docking studies

Based on the network analysis, three therapeutic targets of DM, obesity, and MetS, mainly PPAR-γ, FABP1, and HMGCR, were prioritized, and blind docking was performed for phytocompounds and their respective standard molecules using the following steps. (1) Preparation of ligands: Using the PubChem[18] chemical substance database (https://pubchem.ncbi.nlm.nih.gov/), we obtained the 3D structures of the prioritized ligands (phytocompounds hitting PPAR-γ, FABP1, and HMGCR) in SDF file. The POAP_lig.bash script of the POAP pipeline[19] was executed to minimize the energy of the ligand through the use of the mmff94 force field, and the pose/conformation with the lowest possible energy was chosen. (2) Protein structure validation: the RCSB PDB[20] server was utilized to get the X-ray crystal structures of the prioritized protein molecules, viz., PPARG (PDB ID: 5Y2O), FABP1 (PDB ID: 2F73), and HMGCR (PDB ID: 1HW9). The co-crystallized structures were imported into the CastP[21] and P2Rank[22] servers to retrieve the data on proteins active binding regions. (3) Docking study: AutoDock vina was executed through the POAP_vs.bash script of the POAP pipeline[19] for protein-ligand docking with system exhaustiveness setting to 100. For intermolecular interaction investigations, all produced complexes (with lowest RMSD) were visualized in Discovery Studio Visualizer 2019v.

Molecular dynamics simulation

To learn more about the structural stabilities and intermolecular interactions of the best-docked conformations, we ran an all-atom Molecular Dynamics (MD) simulation of them for 100 ns in explicit solvent with all three targets. We utilized the GROMACS (https://www.gromacs.org/) 2021.3 software[23] package with the

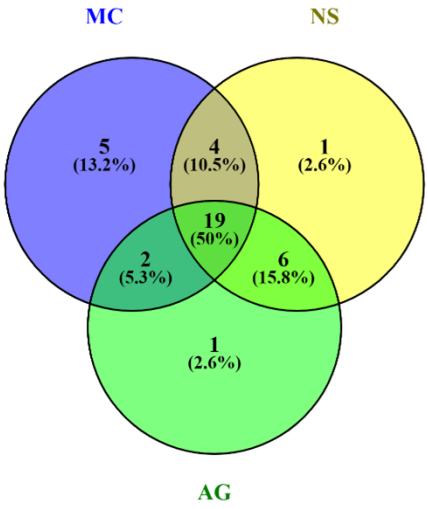

Plant name	Common ger	Gene ID
AG, MC, and NS	19	FABP1 ACE HMGCR G6PD HTR2C CHRM1 ACHE PPARG PTGS1 ADRA2C CA1 CHRM3 HTR2A CHRM2 DRD2 AR MAOB PTGS2 PTGER2
MC and NS	4	HTR1A AGTR1 ADRA1A ADRA1D
AG and MC	2	INSR ACACB
AG and NS	6	PDE5A CHRM4 EDNRA CHRM5 PTGIR MAOA
MC	5	HDAC1 AGTR2 DPP4 MGAM DRD1
NS	1	ADRA1B
AG	1	AOC3

Figure 1: Therapeutic protein targets of MetS modulated by compounds from MC, NS, and AG.

Table 1: Interaction of compounds with PPARG.

Plant name	Compound	Pubchem ID	BE (kcal/mol)	HBI	NHBI
Nigella sativa	Nigellidine	136828302	-7.5	Nil	Ala320, Arg316, Leu256(2), Leu361, Met357(3) Phe254, Pro255,
Nigella sativa	Eicosadienoic-Acid	6439848	-7.2	Arg316	His477, Leu481, Phe310, Tyr501
Momordica charantia	Alpha-Eleostearic-Acid	5281115	-7	His351, Ser317, Tyr351	Phe254, Pro255
Momordica charantia	Stigmasta-7-22-25-Trien-3-Beta-Ol	5283656	-4.6	Nil	Ala320(3), Arg316(3), Cys313(2) His351, His477, Ile354(4), Leu358(6), Leu497, Met357, Phe310(2), Phe391(2), Tyr355
Momordica charantia, Nigella sativa	Alpha-Spinasterol	5281331	-4.5	Nil	Ala320(3), Arg316(3), Cys313(2) His351, His477, Ile354(4), Leu358(6), Leu497, Met357, Met392, Phe310(2), Phe391(2), Tyr355
Anethum graveolens	Gamma-Sitosterol	457801	-4.5	Nil	Ala320(3), Arg316(2), Cys313, Ile354(3), Leu497, Leu358, Met357, Met392, His351(3), His477(2), Phe310, Phe391, Tyr355(2), Tyr501
Nigella sativa	Nigellone	398941	-4.2	Arg316, Cys313, Ser370,	Ala320, Cys313(2), Ile354, Ile367(2), Leu361, Leu381, Met392, Met376(2), Met357(2), Val367(2)
Momordica charantia	Lanosterol	246983	-0.4	Nil	Nil
Nigella sativa	Hederagenin	73299	9.7	Glu323, Leu256	Cys313(3), Ile354, Leu358(3), Leu361(3), Met357(2), Phe391, Tyr355
Momordica charantia	Momordicin	57518366	10.2	Nil	Nil
*Standard	Pioglitazone	4829	-8.7	Ser317, His351, Gln314, Ile354	Cys313, Leu358, Leu256, Leu361, Phe391

BE: Binding energy; HBI: Hydrogen bond interactions; NHBI, Non-hydrogen bond interactions.

Amber ff99SB-ildn force field for executing MD simulations. Topology parameters of the ligands and complete complex were constructed using the xleap module of AmberTools (https://ambermd.org/AmberTools.php), and partial charges of the small molecules were generated by quantum computation in an antechamber[24] using a 'bcc' charge model. In order to solvate the prepared systems, a three-site water (TIP3P) model was used inside a rectangular box with 10.0 Å boundary conditions from the borders of the protein in all directions. The appropriate amounts of counterions were added to the respective systems to neutralize the charges. To find the near-global states with the lowest energy, the steepest descent + conjugate gradient energy minimization approach was applied. Using "canonical (NVT) and isobaric (NPT) ensembles," the systems were allowed to equilibrate for 1 ns. To keep the pressure and temperature (300 K) stable during NVT equilibration, a modified "Berendsen

Table 2: Interaction of compounds with FABP1.

Plant name	Compound	Pubchem ID	BE (kcal/mol)	HBI	NHBI
Nigella sativa	Nigellimine-N-Oxide	69131015	-8.8	Nil	Asn111, Ile52, Phe50
Momordica charantia	Stigmasta-7-22-25-Trien-3-Beta-Ol	5283656	-8.7	Nil	Leu4(3), Leu85(2), Lys46(2), Phe2 (3), Phe48, Val65(2)
Momordica charantia	Lanosterol	246983	-8.1	Nil	Gly66, Leu4, Leu85, Lys46, Phe2(3), Phe48, Val65(2)
Momordica charantia, Nigella sativa	Alpha-Spinasterol	5281331	-8	Nil	Leu4(2), Leu85, Lys46(2), Phe2(3), Val65
Momordica charantia	Alpha-Eleostearic-Acid	5281115	-7.5	Asn61,	Tyr7, Ile41, Ile109
Nigella sativa	Carvone	7439	-7.4	Nil	Asn111, Ile52, Ile 41, Leu71, Leu91(2), Phe63(3), Phe50(3), Thr102, Val83(2)
Momordica charantia	Momordicin	57518366	-7.4	Gly84	Leu85(2), Lys46(4), Phe2(3), Val65(2)
Nigella sativa	Hederagenin	73299	-6.9	Glu68, Lys80, Lys99	Val92, Val82(2), Val 92
Nigella sativa	Eicosadienoic-Acid	6439848	-5.5	Gly45, Ser0(2)	Nil
*Standard	Fenofibric acid	64929	-8.7	Ser39, Arg122, Ser100, Thr102	Thr7, Ile41, Ile109(2), Ile52, Phe50, Leu71(2), Phe95

BE: Binding energy; HBI: Hydrogen bond interactions; NHBI, Non-hydrogen bond interactions.

thermostat algorithm" was used. The "Parrinello-Rahman barostat" was used during NPT equilibration to keep the pressure at 1 bar throughout the process. In addition, the "Particle Mesh Ewald approximation" was used with a cutoff value of 1 nm to calculate "coulomb, van der Waals, and the long-range electrostatic interactions". For bond length constraints, the LINear Constraint Solver method was also employed. The coordinates of all the complexes were recorded at regular intervals of 2 fs throughout a production run lasting 100 ns. The resulting trajectories were analyzed using the embedded gromacs tools and other software programs wherever necessary.

RESULTS

Collection and target identification of bioactives form MC, NS, and AG

Based on the phytochemical databases and literature, 39, 21, 39 compounds from MC, NS, and AG were retrieved, respectively (Supplementary Table 1). Out of 39 from MC, 37 were predicted to modulate about 471 protein targets; 21 compounds from NS were predicted to modulate 387 protein targets; and 39 compounds from AG were predicted to modulate 471 protein targets (Supplementary Table 2).

Compounds targeting to disease related target

From the therapeutic target database, we retrieved 17 protein targets for obesity, 13 for CVD, 55 for hypertension, and 12 for T2DM (Supplementary Table 3). After matching these with phytocompounds modulated targets, 34 compounds from MC were hitting 30 targets associated with obesity, CVD, hypertension, and T2DM. Likewise, 19 compounds from NS were hitting 30 targets and 34 compounds from AG were hitting 28 targets (Supplementary Table 4). Overall, the common genes between Ag, MC, and NS, were 19 (50%); between MC and NS was 4 (10.5%); between MC and AG was 2 (5.3%); and between AG and NS, was 6 (15.8%) (Figure 1).

Gene set pathway and network analysis

The enrichment analysis of 30 target of MC were involved in 23 molecular pathways, of which 20 were associated with MetS (Supplementary Table 5). Likewise, 30 targets of NG were involved in 31 pathways, of which 18 were associated with MetS

(Supplementary Table 6) and 28 targets of AG were involved in 27 pathways, of which 22 were associated with MetS (Supplementary Table 7). Neuroactive ligand-receptor interactions, Calcium, cGMP-PKG, cAMP, AMPK, PI3K-Akt, PPAR, Metabolic signaling pathways, etc. were modulated by compounds. PPARG was the hub gene within the network (Figure 2).

Active site residues information

The active site residues of PPARG (PDB ID: 5Y2O) are Tyr250, Phe254, Pro255, Leu256, Thr257, Lys258, Ile277, Leu283, Gly286, Glu287, Ile290, Phe292, Ile295, Arg308, Ile309, Phe310, Gly312, Cys313, Gln314, Arg316, Ser317, Glu319, Ala320, Glu323, Ile324, His351, Ile354, Tyr355, Met357, Leu358, Ser360, Leu361, Val367, Leu368, Ile369, Ser370, Glu371, Gly372, Met376, Leu381, Phe391, Met392, Lys395, His477, Leu481, Leu493, Leu497, Tyr501. The active site residues of FABP1 (PDB ID: 2F73) are Ser100, Thr102, Ile109, Asn111, Met113, Arg122, Ser124, Ser39, Ile41, Phe50, Ile52, Ile59, Asn61, Phe63, Tyr7, Leu71, Glu72, Thr73, Met74, Val83, Leu91, Thr93, and Phe 95. The active site residues of HMGCR (PDB ID): Glu559, Cys561, Leu562, Lys735, His752, Asn755, Leu853, Leu857.

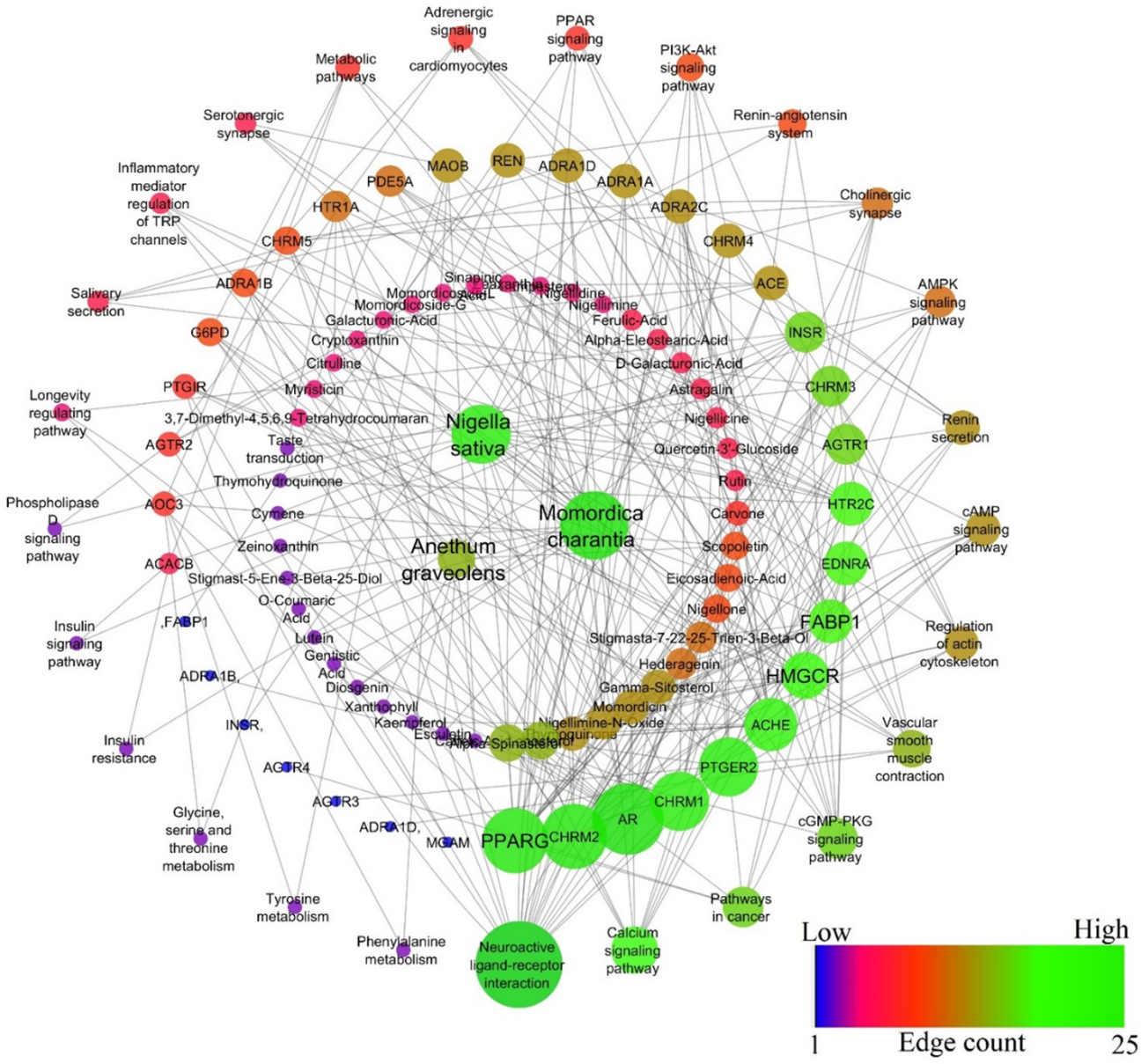

Figure 2: Network representation of phytocompounds from MC, NS, and AG with protein targets and pathways involved in T2DM, obesity, and MetS. Blue color and smaller node size represents compound, protein, and pathway lowest edge count and green color and higher node size represents compound, protein, and pathway highest edge count.

Table 3: Interaction of compounds with HMGCR.

Plant name	Compound	Pubchem ID	BE (kcal/mol)	HBI	NHBI
Momordica charantia	Cryptoxanthin	5281235	-7.1	Val772	Ala754, Pro693, Ala743, Val731(3), Leu857, Lys735
Momordica charantia	Zeaxanthin	5280899	-6.9	Thr558	Val731(2), Lys735, Leu857
Momordica charantia	Lanosterol	246983	-6.7	Asn776	Pro693, Val772, Ala754(4), His752, Leu853(2)
Momordica charantia	Alpha-Spinasterol	5281331	-6.5	Nil	Ala754, Ala772, Ala743
Momordica charantia	Stigmasta-7-22-25-Trien-3-Beta-Ol	5283656	-6.5	Nil	Ala754(3), Ala743, Val772
Momordica charantia	Momordicin	57518366	-6.5	Nil	Ala754(2), Val772, Pro693
Anethum graveolens	Gamma-Sitosterol	457801	-6.3	Nil	Val772(2), Ala754, Ala743, Ser740, Pro693
Anethum graveolens	3,7-Dimethyl-4,5,6,9-Tetrahydrocoumaran	131752931	-4.3	Nil	Pro537, Val563(2)
Momordica charantia	Alpha-Eleostearic-Acid	5281115	-4	Nil	Nil
*Standard	Simvastatin	54454	-6.2	Ser745, Lys735	Ala754(2), Pro693, Gly748

BE: Binding energy; HBI: Hydrogen bond interactions; NHBI, Non-hydrogen bond interactions.

Molecular docking

Among 10 compounds targeting PPARG, Nigellidine scored the least binding energy (-7.5 kcal/mol) with PPARG via forming 10 NHBI with Ala320, Arg316, Leu256(2), Leu361, Met357(3), Phe254, and Pro255. Whereas, standard molecule, Pioglitazone scored the lowest BE of -8.7kcal/mol via forming 4 HBI with Ser317, His351, Gln314, Ile354 and 5 NHBI with Cys313, Leu358, Leu256, Leu361, and Phe391. Among these, Leu256 and Leu361 were common interacting residues for Nigellidine and Pioglitazone. Among 9 compounds targeting FABP1, Nigellimine-N-Oxide scored the lowest BE of -8.8kcal/mol via forming 3 HBI with Asn111, Ile52, Phe50. Whereas, Fenofibric acid scored the lowest BE of -8.7 kcal/mol via forming 4 HBI with Ser39, Arg122, Ser100, Thr102 and 9 NHBI with Thr7, Ile41, Ile109(2), Ile52, Phe50, Leu71(2), Phe95. Among these, Phe50 and Ile52 were common interacting residues for Nigellimine-N-Oxide (NNO) and Fenofibric acid. Likewise, Cryptoxanthin was found to be the lead hit molecule against HMGCR, as it scored the least BE of -7.1 kcal/mol via forming 1 HBI with Val772 and 8 NBHI with Ala754, Pro693, Ala743, Val731(3), Leu857, Lys735. Whereas, standard molecules simvastatin scored the BE of -6.2 kcal/mol and formed 2 HBI with Ser745, Lys735 and 4 NHBI with Ala754(2), Pro693, and Gly748. Among these interactions, Pro693, Lys735, Ala754 were the common interacting residues for Cryptoxanthin and simvastatin. The intermolecular interaction of phytocompounds and respective standard molecules with PPARG, FABP1, and HMGCR were shown in Tables 1-3 and Figure 3.

Molecular dynamics simulation

Stability of Nigellidine and Pioglitazone with PPARG

The complex "Nigellidine- PPARG" and "Pioglitazone- PPARG" showed stable dynamics during the 100ns of simulation after an equilibration period of 18ns (Figure 4). The average backbone RMSDs for Nigellidine and Pioglitazone were ~2.2 Å and ~1.7 Å, and the complex RMSDs were ~2.9 Å and ~2.2 Å, respectively. In the Nigellidine- PPARG complex, the N-terminal residues showed maximum residual fluctuations (~7 Å) compared to pioglitazone-PPARG. However, the residues engaged in the stable and conserved non-bonded interactions Ala320, Arg316, Leu256, Met357, Phe254, Pro255, Ser317, His351, Gln314, Ile354, Cys313, Leu358, Leu361, Phe391 showed relatively smaller fluctuations (~1.5 Å) in both the complexes. In the Nigellidine -PPARG complex, a gradual increase in the Rg value (19 to 19.6 Å) was observed up to ~40ns and found to be stable throughout the simulation period. In the Pioglitazone-PPARG complex, a steady decrease in the Rg value (19.25 to 19.1 Å) was observed up to ~20ns and stable complex formation was seen throughout 100ns. In addition, it was observed that the initial and final average surface areas occupied by pioglitazone with Pparg was ~146

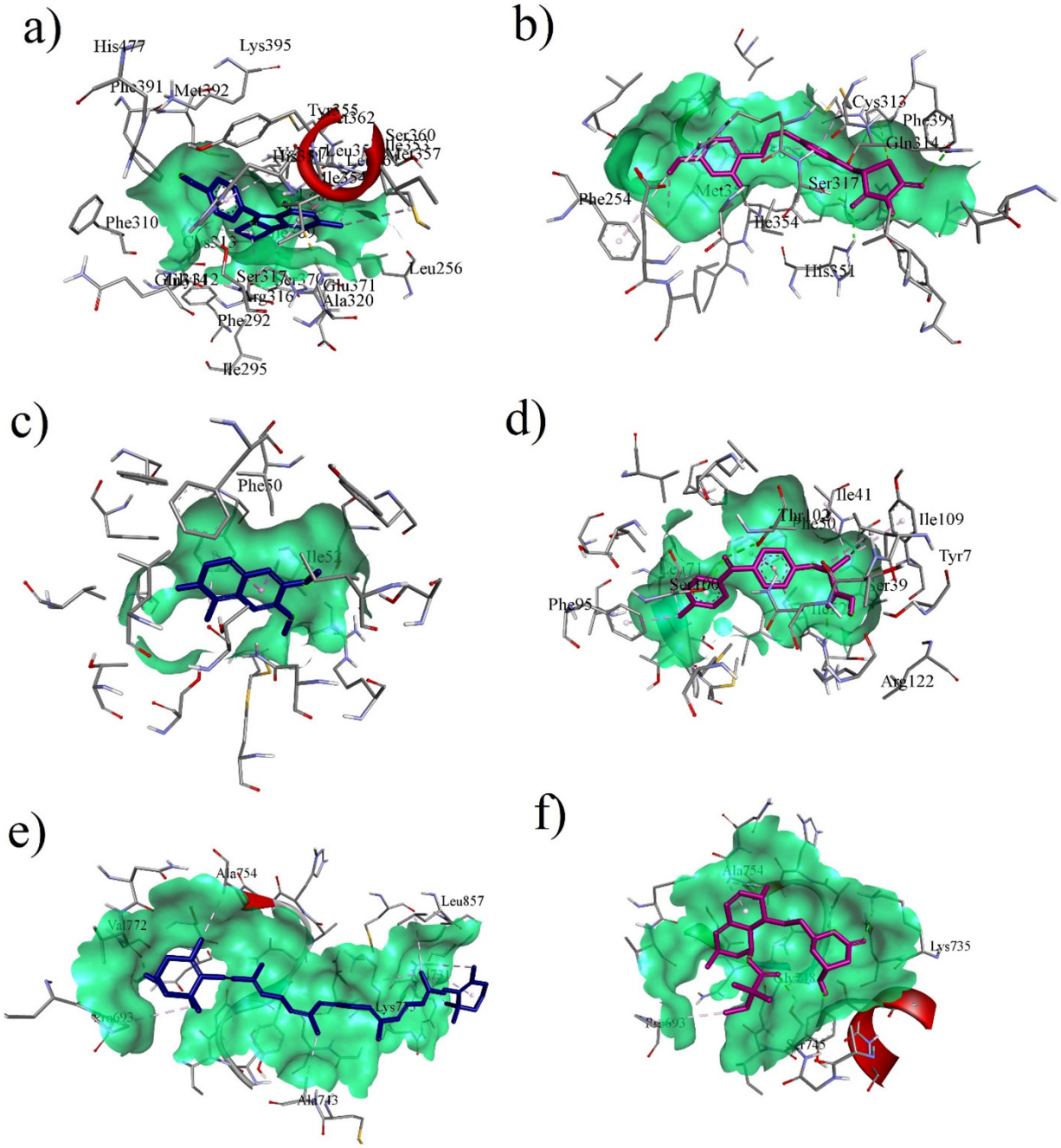

Figure 3: Binding mode of a) Nigellidine and b) Pioglitazone with PPARG; c) Nigellimine-N-Oxide and d) Fenofibric acid with FABP1; e) Cryptoxanthin and f) Simvastatin with HMGCR.

nm^2 and 139.90 nm^2 respectively and the average surface area was ~142 nm^2, which represents higher flexibility of the binding pocket. Nigellidine formed 2 stable H-bonds and Pioglitazone formed 4 H-bonds, of which two were consistent throughout the simulations in both the complexes.

Stability of Nigellimine-N-Oxide (NNO) and Fenofibric acid with FABP1

The complex "NNO-FABP1" showed stable dynamics during the 100ns of simulation compared to and "Fenofibric acid – FABP1" complex (Figure 5). The average backbone RMSDs for NNO and Fenofibric acid were ~1.9 Å and ~2.4 Å, and the complex RMSDs were ~2.2 Å and ~3.0 Å, respectively. In the both the complexes, loop connecting to the beta sheet "Ala54 to Lys57" showed maximum residual fluctuations (~5 Å). However, the residues engaged in the stable and conserved non-bonded interactions Asn111, Ile52, Phe50, Thr7, Ile41, Ile109, Leu71, Phe95 showed relatively smaller fluctuations (~1.4 Å) in both the complexes. In the NNO –FABP1 complex, a stable Rg value (~14.25 Å) was observed up to ~60ns and found to be decrease (14.25 to 14 Å)

and again maintained stability at 14 Å till 100ns. In the Fenofibric acid –FABP1 complex, a stable Rg value (~14.25 Å) was observed up to ~60ns and found to be increase (14.25 to 14.6 Å) and again maintained stability at 14.6 Å till 100ns. A similar trend was observed in the SASA for both the complexes. This indicates a closure of the binding pocket and higher compactness after ~60 ns for NNO-FABP1 complex and opening of the binding pocket and less compactness after ~60 ns for Fenofibric acid -FABP1 complex. NNO formed 4 stable H-bonds of which 3 were consistent throughout the simulations and Fenofibric acid formed 2 H-bonds, of which none were consistent.

Stability of Cryptoxanthin and Simvastatin with HMGCR

The complex "Cryptoxanthin-HMGCR" and Simvastatin-HMGCR showed stable dynamics during the 100 ns of simulation (Figure 6). The average backbone RMSDs for NNO and Fenofibric acid were ~6.2 Å and ~4.5 Å, and the complex RMSDs were ~7.2 Å and ~5 Å, respectively. After an equilibration period of ~30ns, a steady increase in the RMSD were observed throughout 100ns for both the complexes. In the both the complexes, amino acid region "Pro442 to 537" showed maximum residual fluctuations (~2 to ~17 Å). However, the residues engaged in the stable and conserved non-bonded interactions Val772, Ala754, Ala743, Val731, Leu857, Lys735, Ser745, Pro693, and Gly748 showed relatively lesser fluctuations (~2 Å) in both the complexes. The Rg value showed stable complex formation during the MD simulation by forming a compact globular shape as revealed by a steady decrease in the Rg value. A similar trend was observed in the SASA for both the complexes. This indicates a closure of the binding pocket and higher compactness throughout the simulation. Cryptoxanthin formed 2 stable H-bonds of which

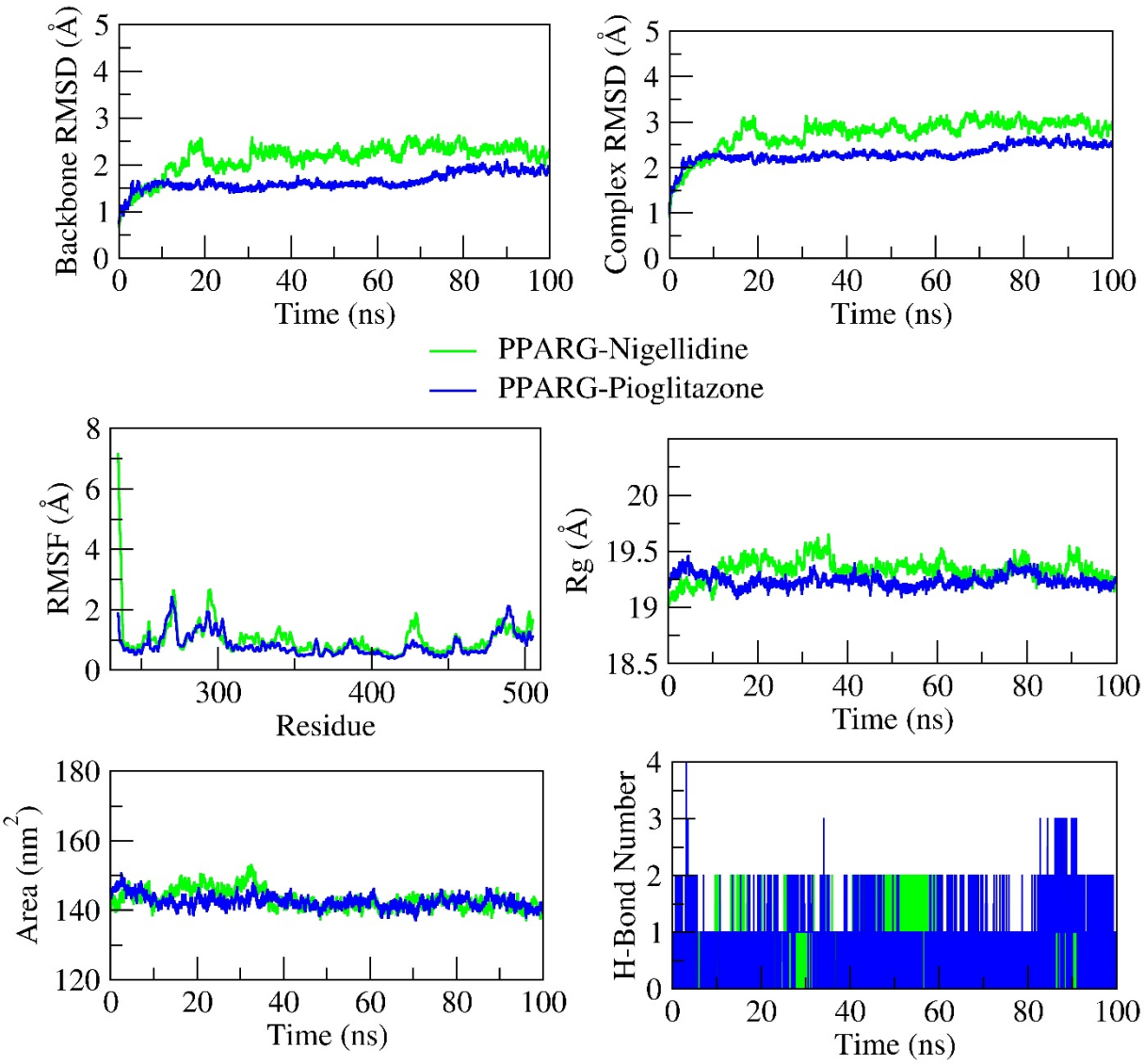

Figure 4: Stability Nigellidine and Pioglitazone with PPARG during 100ns MD simulation. (a) RMSD of backbone, (b) RMSD of complex, (c) RMSF, (d) Rg, (e) SASA, and (f) number of H-bond interactions formed during simulation.

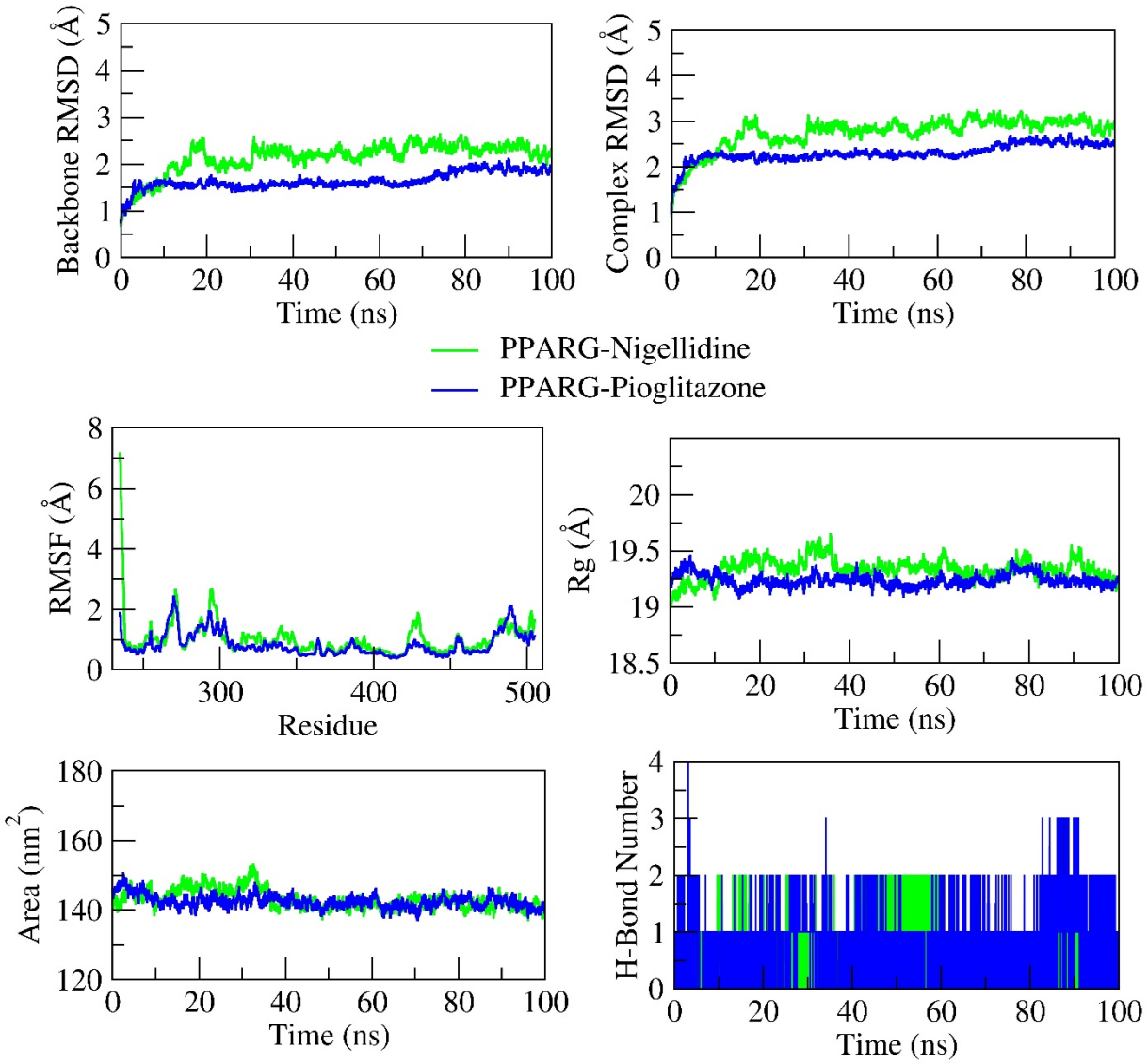

Figure 5: Stability Nigellimine-N-Oxide (NNO) and Fenofibric acid with FABP1 during 100ns MD simulation. (a) RMSD of backbone, (b) RMSD of complex, (c) RMSF, (d) Rg, (e) SASA, and (f) number of H-bond interactions formed during simulation.

1 was consistent throughout the simulations and Simvastatin formed 5 H-bonds, of which 2 were consistent.

DISCUSSION

Momordica charantia (MC), *Nigella sativa* (NS), and *Anethum graveolens* (AG) have been utilized in multiple medicinal applications and have been reported for anti-diabetic and anti-obesity effects in numerous experimental animal models,[25-29] however, their role in the multiple protein targets and pathways and how their compounds work is not yet studied. Due to the complexity and polygenic nature of MetS, reporting its mechanisms is challenging in the presence of various secondary metabolites. Additionally, it is well known that a single compound may affect many proteins. To test this hypothesis, we used multiple *in silico* approaches to identify the probably regulated proteins and pathways that could help to propose the possible therapeutic action of bioactives from three important herbs as well as vegetables (MC, NS, and AG).

To start with, phytocompounds from MC, NS, and AG were retrieved from the phytochemical databases and published in articles. Further, their probable protein targets were identified by SwissTargetPrediction and the predicted set of genes was subjected to pathway enrichment analysis. On the other hand, retrieved the MetS related genes from the TTD and were matched with phytocompounds targets to obtain the only data on phytocompounds targeting MetS related targets (refer to Supplementary Table 4). Interestingly, among the predicted targets, about 50% of the targets were commonly shared between MC, NS, and AG (FABP1, ACE, HMGCR, G6PD, HTR2C, CHRMI, ACHE, PPARG, PTGS1, ADRA2C, CAI, CHRM3, HTR2A, CHRM2, DRD2, AR, MAOB, PTGS2, and PTGER2). Among these, PPARG, FABP1, and HMGCR

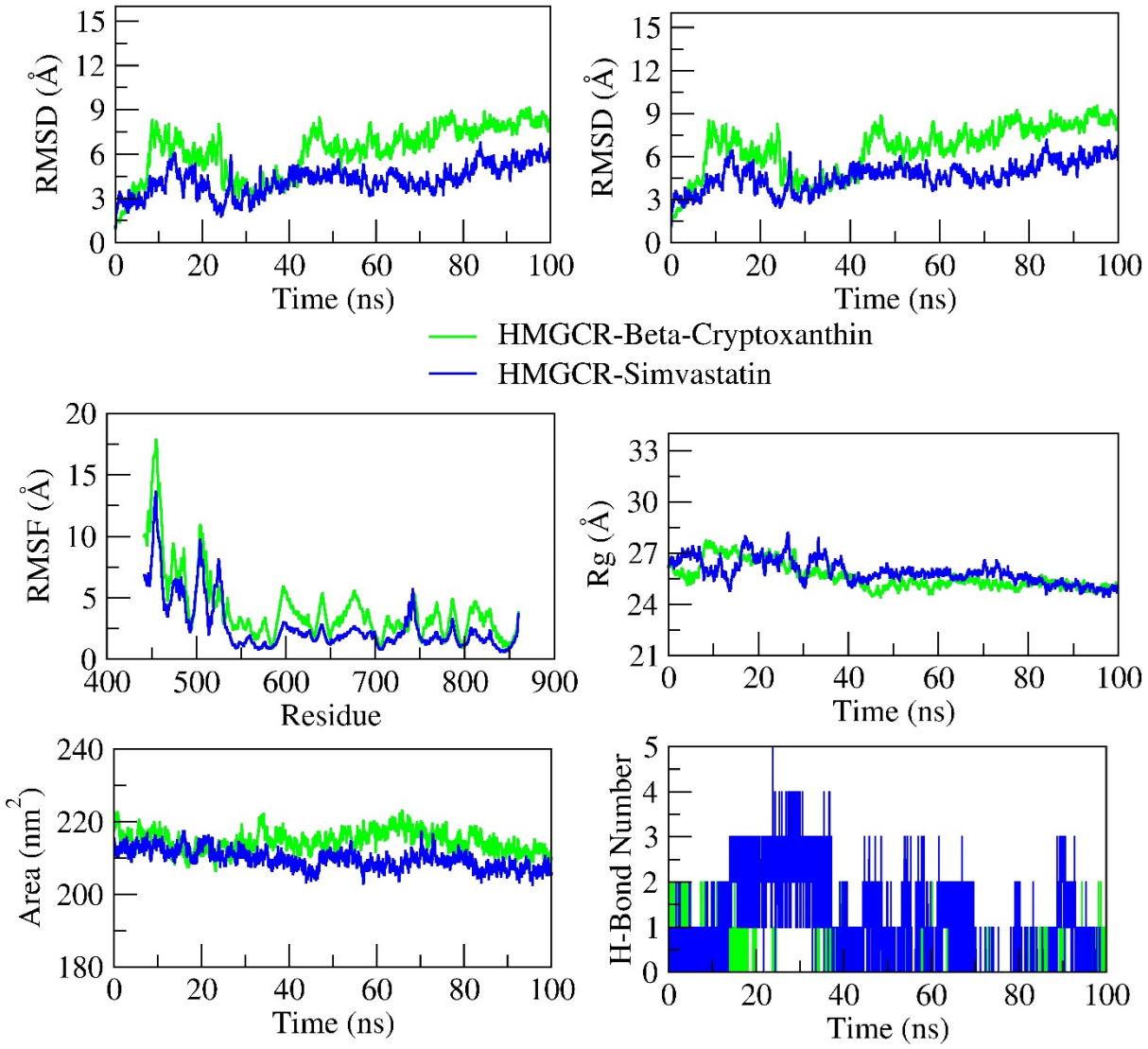

Figure 6: Stability Cryptoxanthin and Simvastatin with HMGCR during 100ns MD simulation. (a) RMSD of backbone, (b) RMSD of complex, (c) RMSF, (d) Rg, (e) SASA, and (f) number of H-bond interactions formed during simulation.

and were the well-known therapeutic targets of MetS, mainly obesity and T2DM. In this study, PPARG was targeted by Nigellidine, Eicosadienoic-Acid, Nigellone, Alpha-Spinasterol, Hederagenin from NS; Alpha-Eleostearic-Acid, Stigmasta-7-22-25-Trien-3-Beta-Ol, Lanosterol, Momordicin from MC; and Gamma-Sitosterol from AG. Similarly, FABP1 was targeted by Nigellimine-N-Oxide, Alpha-Spinasterol, Carvone, Hederagenin, Eicosadienoic-Acid from NS and Stigmasta-7-22-25-Trien-3-Beta-Ol, Lanosterol, Alpha-Eleostearic-Acid, Momordicin from MC. Finally, HMGCR was targeted by Cryptoxanthin, Zeaxanthin, Lanosterol, Alpha-Spinasterol, Stigmasta-7-22-25-Trien-3-Beta-Ol, Momordicin, Alpha-Eleostearic-Acid from MC and Gamma-Sitosterol and 3,7-Dimethyl-4,5,6,9-Tetrahydrocoumaran from AG. The prediction reveals the higher contribution of MC and NS in targeting PPARG, FABP1 and MC and AG in targeting PPARG and HMGCR. We believe that the combination of these three plants could be more effective in modulating PPARG, FABP1, and HMGCR.

PPAR-γ agonists stimulate adipogenesis and speed up the differentiation of adipocytes by increasing Free Fatty Acid (FFA) uptake in subcutaneous adipose tissues.[30] Reducing circulating FFA with a PPAR-γ agonist results in less insulin resistance.[31] Fabp1 is mainly expressed in liver, intestine, pancreas, kidney, lung, stomach. FABPs have access to the nucleus under certain circumstances and may direct fatty acids to transcription factors in the nuclear lumen, such as the PPAR-family members PPAR-α, PPAR-δ and PPAR-γ.[32] By inhibiting the PPAR γ, LXR -α, and pathway of the ATP-binding cassette A1 (ABCA1), FABP reduces cholesterol efflux while regulating inflammatory responses through the IKK-nuclear factor-B (NF-κB) pathway, which leads to the development of obesity and insulin resistance.[32,33] In this study, phytocompounds from all three plants were found to

modulate PPARG and FABP1. Nigellidine from NS scored the BE of -7.5kcal/mol with PPARG via forming interactions with Ala320, Arg316, Leu256, Leu361, Met357, Phe254, and Pro255. Likewise, Nigellimine-N-Oxide from NS scored a BE of -8.8 kcal/mol with FABP1 via interacting with Asn111, Ile52, and Phe50. These compounds showed very stable complex formation with the binding site during 100 ns MD simulation compared to their standard molecules Pioglitazone and Fenofibric acid respectively. On the other hand, HMG-CoA reductase (HMGCR) has crucial regulatory enzyme role in regulating the production of endogenous cholesterol[34] and its inhibitors have an impact on the rate-limiting stage in the production of cholesterol.[35] In this study, Cryptoxanthin from MC scored a BE of -7.1 kcal/mol with HMGCR via forming interaction with Val772, Ala754, Pro693, Ala743, Val731, Leu857, Lys735 and Cryptoxanthin formed a very stable complex formation with the binding site of HMGCR during 100 ns MD simulation compared to its standard molecule Simvastatin.

According to previous studies, NS, MC, and AG prevent apoptosis by upregulating pro-survival signals and downregulating pro-apoptotic signals (PI3K/Akt, JNK, and mTOR signalling) while decreasing inflammation by activating anti-inflammatory signalling (NF-kB and TLR signalling).[36-40] It functions to prime energy metabolism via the AMPK-SIRT1-PGC-1 and PPARg signalling pathways, activate growth factor signalling through the PI3K/Akt pathway, and improve protein clearance by upregulating LRP1.[41] The health advantages of NS, MC, and AG were effected via these processes, including defence against metabolic (obesity, dyslipidemia, and diabetes), cardiovascular and many more complications. In this study, In this study, the phytocompounds from MC, NS, and AG were found to hit therapeutic targets of MetS i.e. FABP1, ACE, HMGCR, G6PD, HTR2C, CHRMI, ACHE, PPARG, PTGS1, ADRA2C, CAI, CHRM3, HTR2A, CHRM2, DRD2, AR, MAOB, PTGS2, PTGER2, HTRIA, AGTRI, ADRAIA, ADRAID, INSR, ACACB, PDE5A, CHRM4, EDNRA, CHRM5, PTGIR, MAOA, HDAC1, AGTR2, DPP4, MGAM, DRD1, ADRA1B, AOC3 and were potentially involved in Neuroactive ligand-receptor interaction, Calcium, PI3K-Akt, cGMP-PKG, cAMP, AMPK, PPAR, Metabolic signaling pathways, etc.

Skeletal muscle plays a crucial role in maintaining steady energy levels and proper glucose metabolism, since it is the primary site of insulin-stimulated glucose utilization (around 90% of the total).[42] Insulin controls skeletal muscle metabolism through the PI3K/AKT signalling pathway, which stimulates glucose transport, glycogen synthesis, and protein synthesis.[43,44] Previous research has shown that preventing the PI3K-AKT pathway from functioning may have a therapeutic effect that is helpful in the treatment of proliferative diabetic retinopathy.[44] In both normal and abnormal cardiac hypertrophy, several studies have shown that the PI3K-AKT pathway regulates cardiomyocyte size, survival, angiogenesis, and inflammation.[44] We found that phytocompounds from MC, NS, and AG to interact with the greatest number of the protein molecules implicated in the development of DM, obesity, and MetS and it was shown that neuroactive ligand-receptor interaction is a key mechanism in the treatment of diabetes and cardioprotection, one of the primary dangers associated with insulin resistance and diabetes. There have been several efforts to use network pharmacology to comprehend the molecular processes of folk remedies in the treatment of complex illnesses.[45] This study investigated traditional drugs for the treatment of complicated disorders like metabolic syndrome by using network pharmacology combined with molecular docking and dynamics studies.

CONCLUSION

The important secondary metabolites/phytoconstituents in the MC, NS, and AG are responsible for the antidiabetic and anti-obesity actions and treat/ reduce the risk of MetS. The identified compounds were found to have interactions with numerous DM-pathogenesis-related protein molecules and pathways. Strong evidence points to a possible function for these potential medical plants in management via regulation of "Neuroactive ligand-receptor interaction, Calcium, cGMP-PKG, cAMP, AMPK, PI3K-Akt, PPAR, Metabolic signaling pathways, etc". In addition, the molecular docking of identified compounds and standard drugs revealed interactions with active site residues of PPARG, FABP1, and HMGCR. The MD simulation for 100 ns inferred higher stability and stronger binding to the active site residues of PPARG, FABP1, and HMGCR than standard molecules. In light of these results, MC, NS, and AG had therapeutic potential against the severe metabolic effects of altered structure and function of PPARG, adipocytes, and lipolysis leading to obesity, T2DM, and MetS.

ACKNOWLEDGEMENT

The authors are thankful to the Principal, KLE College of Pharmacy, Belagavi, KLE Academy of Higher Education and Research, Belagavi, India for supporting this work.

CONFLICT OF INTEREST

The authors declare that there is no conflict of interest.

ABBREVIATIONS

MC: *Momordica charantia*; **NS:** *Nigella sativa*; **AG:** *Anethum graveolens*; **MetS:** Metabolic syndrome; **T2DM:** type 2 diabetes mellitus; **MD:** Molecular dynamics.

Availability of data and materials

All data generated or analyzed during this study are included in this published article [and its supplementary information files].

REFERENCES

1. Rochlani Y, Pothineni NV, Kovelamudi S, Mehta JL. Metabolic syndrome: pathophysiology, management, and modulation by natural compounds. Ther Adv Cardiovasc Dis. 2017;11(8):215-25. doi: 10.1177/1753944717711379, PMID 28639538.
2. Kassi E, Pervanidou P, Kaltsas G, Chrousos G. Metabolic syndrome: definitions and controversies. BMC Med. 2011;9:48. doi: 10.1186/1741-7015-9-48, PMID 21542944.
3. Lin X, Li H. Obesity: epidemiology, pathophysiology, and therapeutics. Front Endocrinol. 2021;12:706978. doi: 10.3389/fendo.2021.706978, PMID 34552557.
4. Vasanthakumar J, Kambar S. Prevalence of obesity among type 2 diabetes mellitus patients in urban areas of Belagavi. Indian J Health Sci Biomed Res (KLEU). 2020;13(1):21-7. doi: 10.4103/kleuhsj.kleuhsj_221_18.
5. Wu Y, Ding Y, Tanaka Y, Zhang W. Risk factors contributing to type 2 diabetes and recent advances in the treatment and prevention. Int J Med Sci. 2014;11(11):1185-200. doi: 10.7150/ijms.10001, PMID 25249787.
6. Lillich FF, Imig JD, Proschak E. Multi-target approaches in metabolic syndrome. Front Pharmacol. 2020;11:554961. doi: 10.3389/fphar.2020.554961, PMID 33776749.
7. Thangavel N, Al Bratty M, Akhtar Javed SA, Ahsan W, Alhazmi HA. Targeting peroxisome proliferator-activated receptors using thiazolidinediones: strategy for design of novel antidiabetic drugs. Int J Med Chem. 2017; 2017:1069718. doi: 10.1155/2017/1069718, PMID 28656106.
8. Patil VS, Deshpande SH, Harish DR, Patil AS, Virge R, Nandy S, *et al.* Gene set enrichment analysis, network pharmacology and *in silico* docking approach to understand the molecular mechanism of traditional medicines for the treatment of diabetes mellitus. J Proteins Proteomics. 2020;11(4):297-310. doi: 10.1007/s42485-020-00049-4.
9. Davies MJ, D'Alessio DA, Fradkin J, Kernan WN, Mathieu C, Mingrone G, *et al.* Management of hyperglycemia in type 2 diabetes, 2018. A consensus report by the American Diabetes Association (ADA) and the European Association for the Study of Diabetes (EASD). Diabetes Care. 2018;41(12):2669-701. doi: 10.2337/dci18-0033, PMID 30291106.
10. Feng H, Chen G, Zhang Y, Guo M. Exploring multifunctional bioactive components from Podophyllum sinense using multi-target ultrafiltration. Front Pharmacol. 2021;12:749189. doi: 10.3389/fphar.2021.749189, PMID 34759823.
11. Ekins S, Mestres J, Testa B. *In silico* pharmacology for drug discovery: methods for virtual ligand screening and profiling. Br J Pharmacol. 2007;152(1):9-20. doi: 10.1038/sj.bjp.0707305, PMID 17549047.
12. Bhattacharya K, Khanal P, Patil VS, Dwivedi PSR, Chanu NR, Chaudhary RK, *et al.* Computational pharmacology profiling of borapetoside C against melanoma. J Biomol Struct Dyn. 2023;11:1-16. doi: 10.1080/07391102.2023.2213333, PMID 37203884.
13. Mohanraj K, Karthikeyan BS, Vivek-Ananth RP, Chand RPB, Aparna SR, Mangalapandi P, *et al.* IMPPAT: A curated database of Indian Medicinal Plants, Phytochemistry and Therapeutics. Sci Rep. 2018;8(1):4329. doi: 10.1038/s41598-018-22631-z, PMID 29531263.
14. Gfeller D, Grosdidier A, Wirth M, Daina, Michielin O, Zoete V. SwissTargetPrediction. SwissTargetPrediction: a web server for target prediction of bioactive small molecules. Nucleic Acids Res. 2014; 42(Web Server issue):W32-8. doi: 10.1093/nar/gku293, PMID 24792161.
15. von Mering CV, Huynen M, Jaeggi D, Schmidt S, Bork P, Snel B. String: a database of predicted functional associations between proteins. Nucleic Acids Res. 2003;31(1):258-61. doi: 10.1093/nar/gkg034, PMID 12519996.
16. Kanehisa M, Furumichi M, Tanabe M, Sato Y, Morishima K. KEGG: new perspectives on genomes, pathways, diseases and drugs. Nucleic Acids Res. 2017;45(D1):D353-61. doi: 10.1093/nar/gkw1092, PMID 27899662.
17. Doncheva NT, Morris JH, Gorodkin J, Jensen LJ. Cytoscape StringApp: network analysis and visualization of proteomics data. J Proteome Res. 2019;18(2):623-32. doi: 10.1021/acs.jproteome.8b00702, PMID 30450911.
18. Kim S, Chen J, Cheng T, Gindulyte A, He J, He S, *et al.* PubChem 2019 update: improved access to chemical data. Nucleic Acids Res. 2019;47(D1):D1102-9. doi: 10.1093/nar/gky1033, PMID 30371825.
19. Samdani A, Vetrivel U. POAP: A GNU parallel based multithreaded pipeline of open babel and AutoDock suite for boosted high throughput virtual screening. Comput Biol Chem. 2018;74:39-48. doi: 10.1016/j.compbiolchem.2018.02.012, PMID 29533817.
20. Burley SK, Berman HM, Kleywegt GJ, Markley JL, Nakamura H, Velankar S. Protein Data Bank (PDB): the single global macromolecular structure archive. *Protein crystallography*. Methods Protoc. 2017:627-41.
21. Tian W, Chen C, Lei X, Zhao J, Liang J. CASTp 3.0: computed atlas of surface topography of proteins. Nucleic Acids Res. 2018;46(W1):W363-7. doi: 10.1093/nar/gky473, PMID 29860391.
22. Krivák R, Hoksza D. P2Rank: machine learning based tool for rapid and accurate prediction of ligand binding sites from protein structure. J Chemoinformatics. 2018:1-2.
23. Abraham MJ, Murtola T, Schulz R, Páll S, Smith JC, Hess B, *et al.* GROMACS: high performance molecular simulations through multi-level parallelism from laptops to supercomputers. SoftwareX. 2015; 1-2: 19-25. doi: 10.1016/j.softx.2015.06.001.
24. Wang J, Wang W, Kollman PA, Case DA. Antechamber: an accessory software package for molecular mechanical calculations. J Am Chem Soc. 2001;222(1).
25. Grover JK, Yadav SP. Pharmacological actions and potential uses of *Momordica charantia*: a review. J Ethnopharmacol. 2004;93(1):123-32. doi: 10.1016/j.jep.2004.03.035, PMID 15182917.
26. Sharma NK, Ahirwar D, Jhade D, Gupta S. Medicinal and phamacological potential of *Nigella sativa*: a review. Ethnobot Leafl. 2009;11.
27. Ahmad A, Husain A, Mujeeb M, Khan SA, Najmi AK, Siddique NA, *et al.* A review on therapeutic potential of *Nigella sativa*: A miracle herb. Asian Pac J Trop Biomed. 2013;3(5):337-52. doi: 10.1016/S2221-1691(13)60075-1, PMID 23646296.
28. Al-Snafi AE. The pharmacological importance of *Anethum graveolens*–A review. Int J Pharm Pharm Sci. 2014;6(4):11-3.
29. Jana S, Shekhawat GS. *Anethum graveolens*: an Indian traditional medicinal herb and spice. Pharmacogn Rev. 2010;4(8):179-84. doi: 10.4103/0973-7847.70915, PMID 22228959.
30. Laplante M, Festuccia WT, Soucy G, Gélinas Y, Lalonde J, Berger JP, *et al.* Mechanisms of the depot specificity of peroxisome proliferator–activated receptor γ action on adipose tissue metabolism. Diabetes. 2006;55(10):2771-8. doi: 10.2337/db06-0551, PMID 17003342.
31. Leonardini A, Laviola L, Perrini S, Natalicchio A, Giorgino F. Cross-talk between PPAR and insulin signaling and modulation of insulin sensitivity. PPAR Res. 2009; 2009:818945. doi: 10.1155/2009/818945, PMID 20182551.
32. Furuhashi M, Hotamisligil GS. Fatty acid-binding proteins: role in metabolic diseases and potential as drug targets. Nat Rev Drug Discov. 2008;7(6):489-503. doi: 10.1038/nrd2589, PMID 18511927.
33. Makowski L, Hotamisligil GS. The role of fatty acid binding proteins in metabolic syndrome and atherosclerosis. Curr Opin Lipidol. 2005;16(5):543-8. doi: 10.1097/01.mol.0000180166.08196.07, PMID 16148539.
34. Afonso MS, Machado RM, Lavrador MS, Quintao ECR, Moore KJ, Lottenberg AM. Molecular pathways underlying cholesterol homeostasis. Nutrients. 2018;10(6):760. doi: 10.3390/nu10060760, PMID 29899250.
35. Balasubramanian R, Maideen NMP. HMG-CoA Reductase Inhibitors (statins) and their drug interactions involving CYP enzymes, P-glycoprotein and OATP transporters-an overview. Curr Drug Metab. 2021;22(5):328-41. doi: 10.2174/1389200222666210114122729, PMID 33459228.
36. Sadeghi E, Imenshahidi M, Hosseinzadeh H. Molecular mechanisms and signaling pathways of black cumin (*Nigella sativa*) and its active constituent, thymoquinone: a review. Mol Biol Rep. 2023;50(6):5439-54. doi: 10.1007/s11033-023-08363-y, PMID 37155017.
37. Hannan MA, Rahman MA, Sohag AAM, Uddin MJ, Dash R, Sikder MH, *et al.* Black cumin (*Nigella sativa* L.): A comprehensive review on phytochemistry, health benefits, molecular pharmacology, and safety. Nutrients. 2021;13(6):1784. doi: 10.3390/nu13061784, PMID 34073784.
38. Nurcahyanti ADR, Jap A, Lady J, Prismawan D, Sharopov F, Daoud R, *et al.* Function of selected natural antidiabetic compounds with potential against cancer via modulation of the PI3K/AKT/mTOR cascade. Biomed Pharmacother. 2021;144:112138. doi: 10.1016/j.biopha.2021.112138, PMID 34750026.
39. Elekofehinti OO, Oyedokun VO, Iwaloye O, Lawal AO, Ejelonu OC. *Momordica charantia* silver nanoparticles modulate S OCS/JAK/STAT and P13K/Akt/PTEN signalling pathways in the kidney of streptozotocin-induced diabetic rats. J Diabetes Metab Disord. 2021;20(1):245-60. doi: 10.1007/s40200-021-00739-w, PMID 34178835.
40. Liu Y, Mu S, Chen W, Liu S, Cong Y, Liu J, *et al.* Saponins of *Momordica charantia* increase insulin secretion in INS-1 pancreatic β-cells via the PI3K/Akt/FoxO1 signaling pathway. Endocrinol Diabetes Nutr (Engl). 2021;68(5):329-37. doi: 10.1016/j.endien.2021.08.004.
41. Cantó C, Auwerx J. PGC-1alpha, SIRT1 and AMPK, an energy sensing network that controls energy expenditure. Curr Opin Lipidol. 2009;20(2):98-105. doi: 10.1097/MOL.0b013e328328d0a4, PMID 19276888.
42. Jaiswal N, Gavin MG, Quinn III WJ, Luongo TS, Gelfer RG, Baur JA, *et al.* The role of skeletal muscle Akt in the regulation of muscle mass and glucose homeostasis. Mol Metab. 2019;28:1-13. doi: 10.1016/j.molmet.2019.08.001, PMID 31444134.
43. Cazarolli LH, Pereira DF, Kappel VD, Folador P, Figueiredo MD, Pizzolatti MG, *et al.* Insulin signaling: a potential signaling pathway for the stimulatory effect of kaempferitrin on glucose uptake in skeletal muscle. Eur J Pharmacol. 2013;712(1-3):1-7. doi: 10.1016/j.ejphar.2013.02.029, PMID 23458067.
44. Huang X, Liu G, Guo J, Su Z. The PI3K/AKT pathway in obesity and type 2 diabetes. Int J Biol Sci. 2018;14(11):1483-96. doi: 10.7150/ijbs.27173, PMID 30263000.
45. Yuan H, Ma Q, Cui H, Liu G, Zhao X, Li W, *et al.* How can synergism of traditional medicines benefit from network pharmacology? Molecules. 2017;22(7):1135. doi: 10.3390/molecules22071135, PMID 28686181.

Cite this article: Chavan RS, Khatib NA, Patil VS. Bioactive Compounds from *Momordica charantia*, *Nigella sativa*, and *Anethum graveolens* against Metabolic Syndrome: Untangling the Complex Relationship. J Young Pharm. 2023;15(4):659-70.